RESEARCH ARTICLE

WILEY

# Platelet-rich plasma counteracts detrimental effect of high-glucose concentrations on mesenchymal stem cells from Bichat fat pad

Vittoria D'Esposito[1,2] | Manuela Lecce[2] | Gaetano Marenzi[3] | Serena Cabaro[1,2] | Maria Rosaria Ambrosio[1,2] | Gilberto Sammartino[3] | Saverio Misso[4] | Teresa Migliaccio[2] | Pasquale Liguoro[2] | Francesco Oriente[2] | Leonzio Fortunato[5] | Francesco Beguinot[1,2] | José Camilla Sammartino[6] | Pietro Formisano[1,2] ⓘ | Roberta Gasparro[3]

[1]URT "Genomics of Diabetes," Institute of Experimental Endocrinology and Oncology, National Research Council, Naples, Italy

[2]Department of Translational Medicine, "Federico II" University of Naples, Naples, Italy

[3]Department of Neuroscience and Reproductive and Odontostomatological Sciences, "Federico II" University of Naples, Naples, Italy

[4]Unit of Transfusion Medicine, ASL-CE, Caserta, Italy

[5]Department of Health Sciences, "Magna Graecia" University of Catanzaro, Catanzaro, Italy

[6]Department of Biology and Biotechnology, "L. Spallanzani" University of Pavia, Pavia, Italy

**Correspondence**
Pietro Formisano, MD, PhD, Department of Translational Medicine, "Federico II" University of Naples, Via Pansini 5, Naples 80131, Italy.
Email: fpietro@unina.it

## Abstract

Diabetic patients display increased risk of periodontitis and failure in bone augmentation procedures. Mesenchymal stem cells (MSCs) and platelet-rich plasma (PRP) represent a relevant advantage in tissue repair process and regenerative medicine. We isolated MSCs from Bichat's buccal fat pad (BFP) and measured the effects of glucose and PRP on cell number and osteogenic differentiation potential. Cells were cultured in the presence of 5.5-mM glucose (low glucose [LG]) or 25-mM glucose (high glucose [HG]). BFP–MSC number was significantly lower when cells were cultured in HG compared with those in LG. Following osteogenic differentiation procedures, calcium accumulation, alkaline phosphatase activity, and expression of osteogenic markers were significantly lower in HG compared with LG. Exposure of BFP–MSC to PRP significantly increased cell number and osteogenic differentiation potential, reaching comparable levels in LG and in HG. Thus, high-glucose concentrations impair BFP–MSC growth and osteogenic differentiation. However, these detrimental effects are largely counteracted by PRP.

**KEYWORDS**

Bichat's buccal fat pad, bone reconstruction, diabetes, mesenchymal stem cells, platelet-rich plasma

---

Vittoria D'Esposito and Manuela Lecce equally contributed to this work.

# 1 | INTRODUCTION

Maxillofacial defects due to trauma, periodontal disease, or cancer resection lead to reduced bone volume and often require bone reconstruction prior to functional rehabilitation. Both the size and the location of the damage may affect bone repair, and the rehabilitation is worsened in the presence of metabolic and/or vascular comorbidities. For instance, it is well established that patients with diabetes mellitus have increased risk of suffering from periodontitis and implant failures, compared with nondiabetic individuals (Morris, Ochi, & Winkler, 2000). In bone augmentation procedures, diabetes is also associated with a significantly increased risk of intraoral bone block graft failure (Schwartz-Arad, Levin, & Sigal, 2005). Similarly, diabetes affects the osteogenesis process in the early phase of guided bone regeneration (Retzepi, Calciolari, Wall, Lewis, & Donos, 2018). In addition, the periodontal therapy and a careful plaque control have been associated with improved glycemic control in type 2 diabetes mellitus (Stewart, Wager, Friedlander, & Zadeh, 2001). Thus, the metabolic impairment occurring in diabetes including chronically elevated levels of blood glucose and of other metabolites may interfere with bone healing. However, a limited amount of studies have directly addressed the effect of metabolic derangements on bone regeneration (Ladha, Sharma, Tiwari, & Bukya, 2017).

Beside chemically engineered biomaterials, several biological approaches have been considered to foster bone reconstruction. These include the use of mesenchymal stem cells (MSCs) and of platelet-derived products.

Mesenchymal stem cells are widely used for the treatment of damaged tissues, following trauma or other pathological culprits (Caplan, 2007). Even though bone marrow represents the mostly used source of MSCs in the clinical field, adipose tissue may serve as a valid alternative (Rezai Rad et al., 2017).

Adipose tissue depots are scattered in several different anatomical regions, as both subcutaneous and visceral fat. The usual sites from which adipose tissue samples are collected for regenerative medicine purposes are abdomen, breast, knee, and thigh. Maxillofacial applications have arisen the possibility to use Bichat's buccal fat pad (BFP) as source of MSCs. BFP is a deep fat pad located on either side of the face between the buccinators and several superficial muscles, including the masseter and the zygomatic major and minor muscles (Yousuf et al., 2010). It is easy to harvest and provides a proper quantity of tissue for cell isolation (Salehi-Nik et al., 2017). MSCs from BFP (BFP–MSCs) display a phenotype similar to those derived from subcutaneous adipose tissue (sc-MSCs). Analogous to sc-MSCs, BFP–MSCs express defined MSC markers and are able to differentiate into several cell lineages in the presence of specific stimuli (Broccaioli et al., 2013; Farre-Guasch, Marti-Page, Hernandez-Alfaro, Klein-Nulend, & Casals, 2010).

Changes in systemic and local microenvironment, like those of diabetes mellitus, may compromise MSC intrinsic functions. Indeed, insulin resistance, hyperglycemia, persistent inflammation, increased oxidative stress, and the accumulation of advanced glycation end products affect proliferation, differentiation, angiogenic capability, and cytokine secretion of MSCs from bone marrow and subcutaneous adipose tissue (Fijany et al., 2019; van de Vyver, 2017). The effect of metabolic derangements on BFP–MSCs, however, has never been explored.

Platelet products are widely used in all medical fields that require tissue regeneration due to the positive effects in acceleration and promotion of wound healing, reduction of bleeding, and regeneration of soft and hard tissues (Burnouf et al., 2013; Cabaro et al., 2018). During normal tissue repair, platelets release high concentrations of proteins involved in cell proliferation, chemotaxis, and extracellular matrix production/angiogenesis, such as platelet-derived growth factor (PDGF), transforming growth factor β (TGF-β), and vascular endothelial growth factor (VEGF). The healing process is achieved also through the release of a number of cytokines and chemokines, among which C–C motif ligand 5 (CCL5), interleukin (IL)-1β, IL-8, and macrophage inflammatory protein (MIP)-1α (Cabaro et al., 2018; Lacci & Dardik, 2010; Lubkowska, Dolegowska, & Banfi, 2012) play a crucial role. in vivo studies reported that the cotransplantation of platelet-rich plasma (PRP) and sc-MSCs significantly improved bone regeneration (Tobita, Tajima, & Mizuno, 2015). in vitro studies showed a stimulatory effect of PRP in increasing growth and motility of sc-MSCs (D'Esposito et al., 2015; Xu et al., 2015). However, PRP effect on BFP-isolated MSCs has not been determined.

Thus, the aim of this study was to evaluate the impact of high concentrations of glucose and PRP on BFP–MSCs proliferation and osteogenic differentiation in comparison with sc-MSCs. This is a relevant issue because the knowledge of BFP–MSC response to high-glucose concentration and to PRP stimuli may point out new challenges for BFP–MSC-based therapies for oral bone reconstruction.

# 2 | MATERIALS AND METHODS

## 2.1 | Bichat's fat pad sample collection and PRP preparation

Samples of BFP were harvested from nine patients (M/F: 4/5; mean age 37.5 ± 3.5 years) undergoing to maxillary bone reconstruction interventions using BFP as biological vascularized membrane (Choi & Lee, 2016). Patients did not display any metabolic and immunological diseases and were not diagnosed with any form of cancer. Fat specimens were obtained at the end of maxillary bone reconstruction by the same surgeons using sterile tweezers and scissors. Samples were immediately sent to the laboratory for cell isolation.

For plasma collection, four healthy blood donors (M/F: 4/0; mean age 31.5 ± 6.24 years) were enrolled in the study. All were nonsmokers, nonobese (body mass index mean 23.68 ± 3.42), and with a platelet count more than 200,000/μl. Blood was drawn from each subject and was collected in a Vacutainer tube (Vacutainer; Becton Dickinson, East Rutherford, NJ, USA) containing 10% trisodium citrate anticoagulant solution for the preparation of PRP. Venous whole blood was initially centrifuged at 350 g for 15 min, and the supernatant transferred into another tube for a second centrifugation step for

10 min at 980 $g$. After centrifugation, the upper fraction, containing platelet poor plasma, was discarded, and the lower fraction, containing PRP, was used for the experimental procedures (Passaretti et al., 2014). The platelet density was increased by threefold in PRP compared with that in the original venous whole blood. For platelet gel preparations, the sample was incubated for 1 h at 37°C with calcium gluconate (Galenica Senese—10-mg/ml final concentration) to allow clot formation (Giacco et al., 2006). Informed consent was obtained from every subject before the procedure. Both procedures were approved by the ethical committee of the University of Naples (Prot. N. 89/15).

## 2.2 | Cell isolation and growth

Adipose tissue specimens were chopped into small pieces and enzymatically digested by collagenase solution (1 mg/ml—Sigma-Aldrich, St. Louis, MO, USA) for 1 h at 37°C. The stromal vascular fraction containing MSCs was obtained by centrifugation at 1,200 $g$ for 5 min and plated in regular Dulbecco's modified Eagle's medium (DMEM)—F12 (1:1) supplemented with 10% fetal bovine serum, 2-mM glutamine, 100-unit/ml penicillin, and 100-unit/ml streptomycin (Lonza Group Ltd, Basel, Switzerland) (D'Esposito et al., 2012). For growth evaluation, $1 \times 10^4$ BFP–MSCs were seeded in 12-well culture plates. The following day, the cells were starved in serum-free medium supplemented with 0.25% bovine serum albumin for 9 h before the incubation with specific stimuli. After 48 and 72 h, cells were counted either by Neubauer chamber or with the TC10™ automated cell counter (Bio-Rad, Hercules, CA, USA) according to the manufacturer's protocol.

## 2.3 | Flow cytometry analysis

Expression of mesenchymal markers on isolated cells was analyzed by flow cytometry. A total of $2 \times 10^5$ BFP–MSCs were suspended in 200-μl phosphate-buffered saline for analysis. Cells were incubated with PE-conjugated anti-CD73 antibody, FITC-conjugated anti-CD90 antibody, APC-conjugated anti-CD31 antibody, and APC-Cy7-conjugated anti-CD45 antibody as well as dye/isotype-matched antibodies (all from BD Biosciences, San Jose, CA, USA) in dark environment for 30 min at 4°C. Afterward, unbound antibodies were washed out, and the samples were processed by a BD LSR Fortessa (BD Biosciences, San Jose, CA, USA) and analyzed using BD FACS Diva software. $10^4$ events for each sample were acquired in all analyses. Cells were counted and compared with the signals of the corresponding antibody isotype controls.

## 2.4 | Cell differentiation

Cells were seeded at a density of $5 \times 10^4$ cells in 24-well plates, and once the cultures were 100% confluent (2 days), an appropriate differentiation mix was added. Adipogenic differentiation was performed as previously described (Isakson, Hammarstedt, Gustafson, & Smith, 2009) and assessed by lipid accumulation using Oil Red O staining (Sigma-Aldrich, St. Louis, MO, USA) (Ramirez-Zacarias, Castro-Munozledo, & Kuri-Harcuch, 1992). Osteogenic differentiation was performed as previously described (Lanza et al., 2015) and assessed by detection of mineralization foci using Alizarin Red S (ARS) staining (Sigma-Aldrich, St. Louis, MO, USA). Briefly, cells were fixed with 4% formaldehyde for 15 min, washed with bidistilled water (bdH$_2$O), and stained with ARS pH 4.1 for 20 min at room temperature with gentle shaking. Then, the unincorporated dye was removed, and cells were washed with bdH$_2$O. Images of stained monolayers were taken by the Olympus DP20 microscope digital camera system (Olympus Corporation, Tokyo, Japan). For quantification, 800-μl 10% acetic acid was added to each well. Cell monolayers were scraped and transferred to a 1.5-ml microcentrifuge tube. After vortexing for 30 s, tubes were heated at 85°C for 10 min, transferred on ice for 5 min, and centrifuged at 20,000 $g$ for 15 min. A 500 μl of the supernatant was removed and transferred to a new tube, and a 200 μl of 10% ammonium hydroxide was added to neutralize the acid. ARS staining was assessed by optical density determination at 405 nm using a microplate reader (Lanza et al., 2015). The osteogenic differentiation was evaluated also by the assessment of alkaline phosphatase (ALP) specific activity, as indicated below.

## 2.5 | ALP activity

Alkaline phosphatase activity was evaluated upon 14 days from the induction of the osteogenic differentiation. Intracellular enzyme activity was determined by measuring the cleavage of 10-mM p-nitrophenylphosphate at 405 nm using a commercially available kit (BioVision, Inc., CA, USA). Total ALP activity was expressed as nmol p-nitrophenylphosphate hydrolysed/min.

## 2.6 | Real-time and reverse transcription polymerase chain reaction analysis

Total RNA was isolated from cells using Trizol solution (Life Technologies, Carlsbad, CA, USA) according to the manufacturer's instructions. All RNA samples were quantified by measuring the absorbance at 260 and 280 nm (NanoDrop spectrophotemeter, Life Technologies, Carlsbad, CA, USA). For real-time reverse transcription polymerase chain reaction (RT-PCR) analysis, 1-μg RNA was reverse transcribed using SuperScript III reverse transcriptase (Life Technologies, Carlsbad, CA, USA). PCR was analyzed using SYBR Green mix (Bio-Rad, Hercules, CA, USA). Reactions were performed using Platinum SYBR Green Quantitative PCR Super-UDG using an iCycler IQ multicolor real-time PCR detection system (Bio-Rad, Hercules, CA, USA). All reactions were performed in duplicate, and peptidylprolyl isomerase A (PPIA) was used as an internal standard. Primer pair sequences are listed in Table 1.

**TABLE 1** Primer pairs used for quantitative real-time polymerase chain reaction

| Gene | Primer forward | Primer reverse | Product size |
|---|---|---|---|
| ALP | 5′ TAAGGACATCGCCTACCAGC 3′ | 5′ TCTTCCAGGTGTCAACGAGG 3′ | 170 BP |
| PPIA | 5′ TACGGGTCCTGGCATCTTGT 3′ | 5′ GGTGATCTTCTTGCTGGTCT 3′ | 196 BP |
| RUNX2 | 5′ TCTTCAGCACAGTGACACCA 3′ | 5′ TCACGTCGCTCATTTTGCC 3′ | 111 BP |
| COL1A1 | 5′ GGCCCAGAAGAACTGGTACA 3′ | 5′ CGCTGTTCTTGCAGTGGTAG 3′ | 496 BP |

## 2.7 | Immunoblot procedure

Total cell lysates were obtained and separated by sodium dodecyl sulphate–polyacrylamide gel electrophoresis as previously described (Ariemma et al., 2016). Briefly, cells were solubilized for 20 min at 4°C with lysis buffer containing 50-mM HEPES, 150-mM NaCl, 10-mM EDTA, 10-mM $Na_4P_2O_7$, 2-mM sodium orthovanadate, 50-mM NaF, 1-mM phenylmethylsulfonyl fluoride, 10-μg/ml aprotinin, 10-μg/ml leupeptin, pH 7.4, and 1% (v/v) Triton X-100. Lysates were clarified by centrifugation at 12,000 *g* for 20 min at 4°C. The protein concentrations in the cell lysates were measured using a Bio-Rad detergent compatible assay. Proteins were separated by sodium dodecyl sulphate–polyacrylamide gel electrophoresis and blotted on Immobilon-P membranes (Millipore, Billerica, MA, USA). Membranes were blocked for 1 h in TBS (10-mM Tris–HCl, pH 7.4, and 140-mM NaCl) containing 3% (w/v) bovine serum albumin and then incubated with the following antibodies: anti-RUNX2 (1:100, Lot J1118; Santa Cruz Biotechnology, CA, USA), anti-Collagen type I (1:200, Lot L0505; Santa Cruz Biotechnology, CA, USA), and anti-Vinculin (1:5,000, Lot K2116; Santa Cruz Biotechnology, CA, USA). Detection of blotted proteins was performed by EuroClone (ECL SpA, Milan, Italy) according to the manufacturer's instruction. Densitometric analysis was performed using Image Lab software (Bio-Rad, Hercules, CA, USA).

## 2.8 | Statistical analysis

Data were analyzed with GraphPad Prism 6.0 software (GraphPad Software Inc., La Jolla, CA, USA) by unpaired two-tailed *t* test and one-way ANOVA, followed by Sidak's multiple comparison tests. *p* value of less than 0.05 was considered statistically significant.

## 3 | RESULTS

### 3.1 | Isolation and characterization of BFP–MSCs

Mesenchymal stem cells were isolated from Bichat's fat pad (BFP–MSCs) and formed a monolayer of large flat cells exhibiting fibroblast-like shape (Figure 1a). After initial plating, BFP–MSCs had a lag period of about 48 h; then, they started to grow, and their doubling time was 24 h in regular culture medium, although in the absence of serum, their number was significantly reduced (Figure 1b). BFP–MSCs were characterized for immunophenotype and for adipogenic and
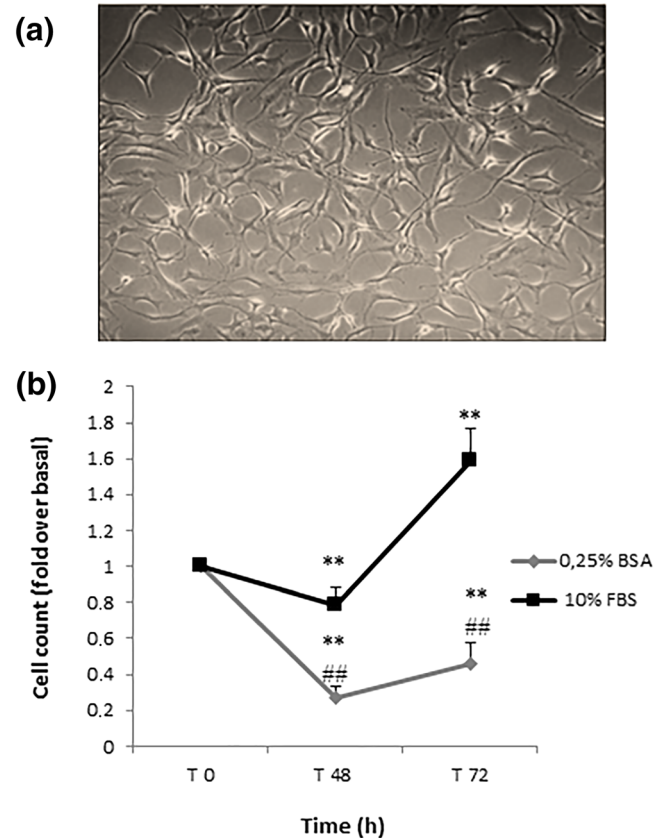


**FIGURE 1** Isolation and growth of mesenchymal stem cell (MSC) from Bichat fat pad. (a) Representative image of MSC isolated from Bichat fat pad biopsies (magnification 10×). (b) BFP–MSCs were incubated in DMEM F12 with 10% FBS or 0.25% bovine serum albumin for 48 and 72 h. Cells were counted, and the results were reported as cell number relative to Day 0 (T0). Data in the graphs represent the mean ± SD of at least three experiments. Asterisk (*) denotes statistically significant values over T0 (**$p \le 0.01$). Sign number (#) denotes statistical significance versus 10% FBS (##$p \le 0.01$) [Colour figure can be viewed at wileyonlinelibrary.com]

osteogenic differentiation potential. As shown in Figure 2a, cells stained positively for mesenchymal progenitor cell surface antigens CD90 and CD73, whereas they stained negatively for CD45 and CD31, hematopoietic and endothelial markers, respectively. In the presence of adipogenic stimuli, BFP–MSCs shifted from a fibroblast-like appearance to a rounded cell phenotype, containing vacuoles-enriched cytoplasm. Oil Red O staining indicated the presence of large and clear lipid droplets occurring in differentiated cells, appearing as mature adipocytes (Figure 2b). Osteogenic differentiation was also
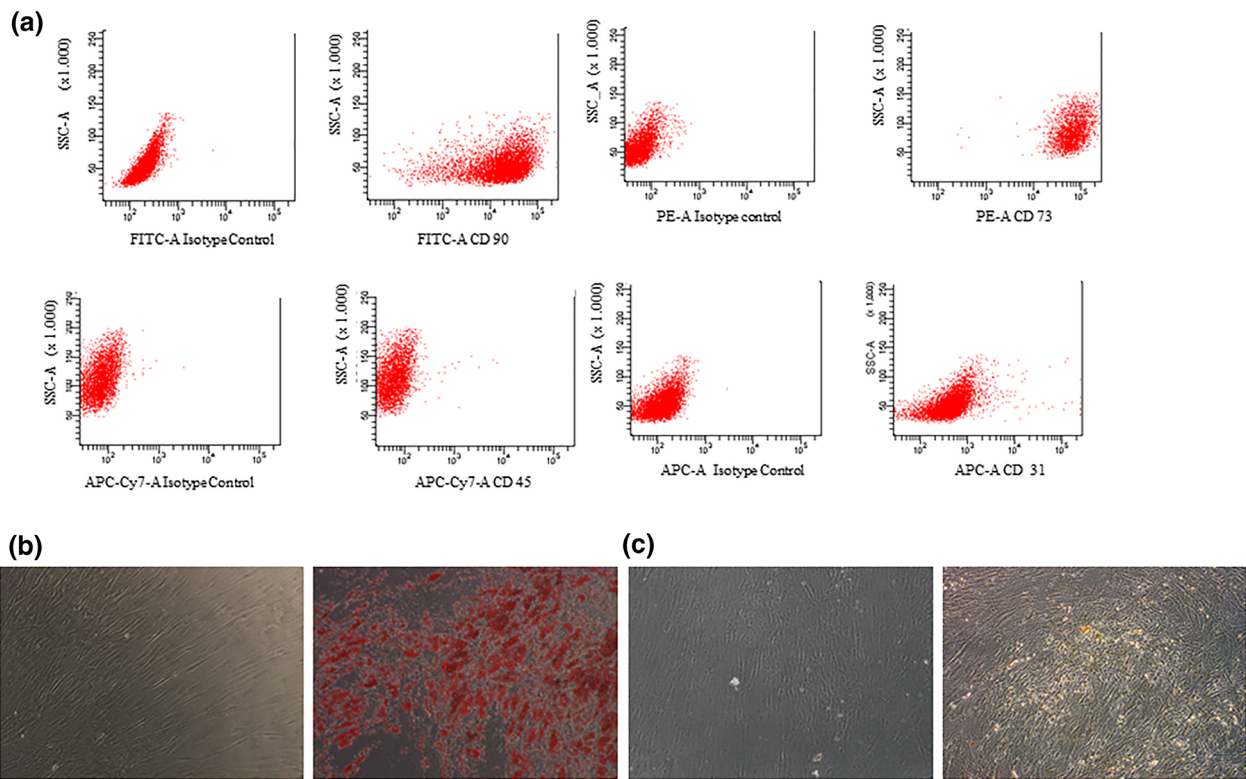
**FIGURE 2** Characterization of BFP–MSCs. (a) Representative dot plots from FACS analysis of BFP–MSCs stained for CD 90, CD 73, CD 45, and CD 31 antigens. (b) Representative microscopic images (magnification 10×) from Oil Red O staining for lipid accumulation detection. (c) Representative microscopic images (magnification 10×) from ARS staining for calcium accumulation detection [Colour figure can be viewed at wileyonlinelibrary.com]

successfully induced in BFP–MSCs when cultured in osteogenic medium. Indeed, the cells displayed detectable calcium accumulation, as shown by ARS staining (Figure 2c).
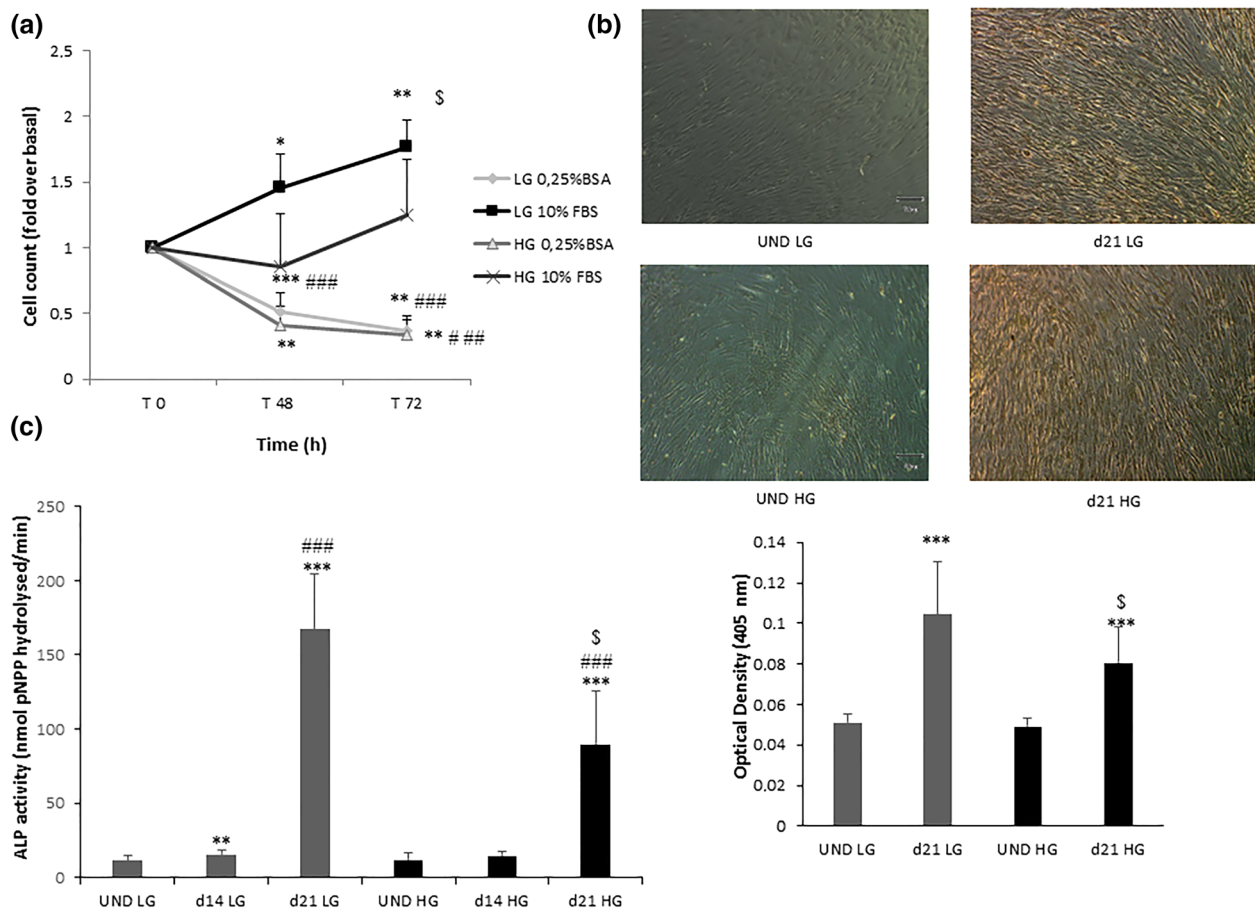
## 3.2 | Effect of glucose on BFP–MSC proliferation and osteogenic differentiation

Next, the effect of high concentrations of glucose was evaluated on proliferation and osteogenic differentiation of BFP–MSCs. To this end, cells were cultured in 5.5-mM glucose (low glucose [LG]), corresponding to near-normal fasting glucose levels in humans, or in 25-mM glucose (high glucose [HG]), resembling hyperglycemia. As shown in Figure 3a, serum deprivation reduced BFP–MSC number both in LG and in HG, whereas in the presence of serum, only in LG, cell number was increased by 1.5-fold and twofold upon 48 and 72 h, respectively. The number of BFP–MSCs was significantly higher when cultured in LG and then in HG, at both 48 and 72 h (Figure 3a). Notably, BFP–MSC proliferation rate with and without serum was similar to that observed for subcutaneous adipose-derived sc-MSCs (Figure S1a and Data S1). However, no differences were found comparing sc-MSC proliferation in HG to LG (Figure S1a and Data S1).

To study the effect of glucose on BFP–MSCs osteogenic differentiation potential, cells were treated with osteogenic stimuli (as described in Section 2), either in LG or in HG medium for 21 days. ARS staining

showed that, at Day 21, after induction of differentiation, BFP–MSCs displayed detectable calcium accumulation both in LG and in HG (Figure 3b). However, ARS quantification indicated that a significantly greater amount of calcium was deposited in LG compared with HG (Figure 3b). ALP activity was also evaluated. As shown in Figure 3c, ALP activity significantly increased in LG already upon 14 days from the induction of differentiation, whereas in HG, no differences were found between undifferentiated controls and differentiated cells. Upon 21 days, a 10-fold and a 6.3-fold increase in ALP activity were observed in LG and in HG, respectively. However, ALP activity was 1.8-fold higher in LG compared with HG (Figure 3c). Differently, from BFP–MSCs, in sc-MSCs, a relatively slight greater amount of ARS was detected in HG (Figure S1b and Data S1). No differences were found in ALP activity between HG and LG (Figure S1c and Data S1).

To further clarify the effect of high-glucose concentration on BFP–MSCs, mRNA levels of *ALP*, *RUNX2*, and *COL1A1* were determined by qRT-PCR after 2 and 21 days upon the induction of differentiation (Figure 4a–c). *RUNX2* is considered the master osteoblast-specific transcription factor, even if several other factors control the entire process. Among these, *ALP* is an early marker of osteogenic differentiation, and *COL1A1* is instrumental to terminal differentiation (Dalle Carbonare, Innamorati, & Valenti, 2012). Results showed that, in LG, *ALP* mRNA levels were significantly increased at Day 2 and still higher at Day 21; at variance, in HG, only at Day 21, a significant increase of *ALP* mRNA
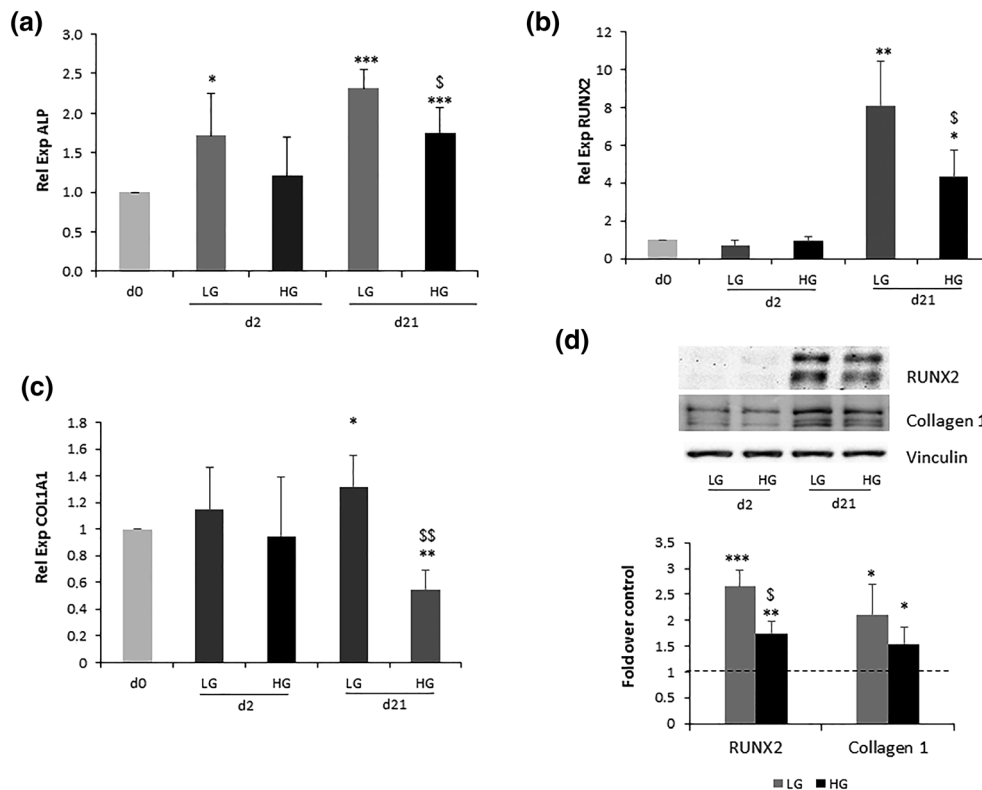
**FIGURE 3** Effect of glucose on BFP–MSC proliferation and differentiation. (a) BFP–MSCs were incubated in DMEM 5.5-mM glucose (low glucose [LG]) or 25-mM glucose (high glucose [HG]) supplemented with 10% FBS or 0.25% bovine serum albumin for 48 and 72 h. Cells were counted as described in Section 2, and the results were reported as cell number relative to T0. Asterisk (*) denotes statistical significance over T0 (*$p \leq 0.05$; **$p \leq 0.01$; ***$p \leq 0.001$). Number sign (#) denotes statistical significance versus 10% FBS (###$p \leq 0.001$). Dollar sign ($) denotes statistical significance versus HG ($$p \leq 0.05$). (b and c) BFP–MSCs were cultured in osteogenic differentiation medium in LG or HG for 21 days. Alizarin Red S representative images at 10× magnification (upper) and quantification (lower). Data in the graphs represent the mean ± SD of at least five experiments. Asterisk (*) denotes statistical significance versus undifferentiated cells (***$p \leq 0.001$). Dollar sign ($) denotes statistical significance versus LG ($$p \leq 0.05$) (b) and (c) ALP activity. Data in the graphs represent the mean ± SD of at least four experiments. Asterisk (*) denotes statistical significance versus undifferentiated cells (**$p \leq 0.01$; ***$p \leq 0.001$). Number sign (#) denotes statistical significance versus Day 14 (###$p \leq 0.001$). Dollar sign ($) denotes statistical significance versus LG ($$p \leq 0.05$) [Colour figure can be viewed at wileyonlinelibrary.com]

levels was observed. Interestingly, at Day 21, the expression levels of *ALP* were significantly lower in HG medium, compared with LG medium (Figure 3a). *RUNX2* mRNA levels were increased at Day 21 either in LG and in HG. However, *RUNX2* mRNA levels were twofold lower in HG than in LG (Figure 4b). *COL1A1* mRNA levels were increased at Day 21 only in LG, whereas in HG, a significant reduction was observed compared either with undifferentiated cells or with cells differentiated in LG (Figure 4c). Finally, protein levels of RUNX2 and Collagen 1 were assessed by western blot after 2 and 21 days upon the induction of differentiation (Figure 4d). As shown, at Day 2, RUNX2 levels were undetectable, whereas Collagen 1 levels were similar in LG and HG. At Day 21, significantly higher levels of RUNX2 and Collagen 1 were detected compared with Day 2 (Figure 4d). Moreover, at Day 21, higher levels of RUNX2 and Collagen 1 were observed in LG compared with HG (Figure 4d).

## 3.3 | Effect of PRP on BFP–MSC proliferation and differentiation

It has been previously reported that PRP promotes proliferation and osteogenic differentiation of sc-MSCs (D'Esposito et al., 2015). We tested, therefore, the hypothesis that PRP may restore BFP–MSC growth in the presence of high concentration of glucose.

At first, the effect of PRP on cell proliferation and osteogenic differentiation was determined in the standard growth medium (DMEM-F12). In the absence of bovine serum, 10% PRP (v/v in DMEM-F12) increased cell number by 1.5-fold and fourfold upon 48 and 72 h, respectively (Figure S2a and Data S1). PRP further increased cell proliferation also in the presence of 10% serum (data not shown). In the same conditions, as indicated by the determination of *ALP* mRNA levels, PRP treatment did not modify cell osteogenic potential (Figure S2b and Data S1).

**FIGURE 4** Effect of glucose on BFP–MSC osteogenic markers. BFP–MSCs were cultured in osteogenic differentiation medium in low glucose (LG) or high glucose (HG) for 21 days. *ALP* (a), *RUNX2* (b), and *COL1A1* (c) mRNA levels were determined by real-time RT-PCR analysis. Data have been normalized on PPIA as internal standard. Bars show the mRNA levels relative to undifferentiated control. Data in the graphs represent the mean ± SD of at least four experiments. Asterisk (*) denotes statistical significance versus undifferentiated cells (***$p \leq 0.001$). Dollar sign ($) denotes statistical significance versus LG ($$p \leq 0.05$; $$$p \leq 0.01$). (d) Cell lysates (30-µg protein/sample) were blotted with RUNX2 and Collagen 1 antibodies. To ensure the equal protein transfer, membranes were blotted with vinculin antibodies. Filters were revealed by ECL and autoradiography. The autoradiographs shown are representative of three independent experiments. Densitometric analysis has been performed on autoradiographs. Bars show the ratio RUNX2/vinculin and Collagen 1/vinculin protein levels relative to control (cells at Day 2), represented as dotted line. Data in the graphs represent the mean ± SD of three experiments. Asterisk (*) denotes statistical significance versus control (***$p \leq 0.001$; **$p \leq 0.01$; *$p \leq 0.05$). Dollar sign ($) denotes statistical significance versus LG ($$p \leq 0.05$)

We next evaluated the effect of PRP on cell growth and osteogenic differentiation potential in the presence of LG and HG medium. In LG, PRP increased cell number by 2.5-fold and 4.5-fold, after 48 and 72 h, respectively. Interestingly, in HG, 10% serum had almost no effect, whereas 10% PRP increased cell proliferation by 2.5 fold at 72 h (Figure 5a). In sc-MSCs, PRP induced a significant increase of cell growth compared with untreated cell, without any difference between LG and HG (Figure S3a and Data S1).

Alizarin Red S staining showed that PRP promoted osteogenic differentiation in BFP–MSCs both in LG and in HG (Figure 5b). However, in HG, PRP-treated cells showed 1.3-fold less calcium accumulation compared with PRP-treated cells in LG (Figure 5b). Moreover, in LG, PRP increased ALP activity by 1.4-fold compared with cells differentiated without PRP (Figure 5c). In HG, PRP induced an increase of ALP activity at Day 14, where no differences were found between undifferentiated controls and differentiated cells (without PRP) (Figure 5c). However, ALP activity in HG was significantly lower than in LG (Figure 5c). In sc-MSCs, as expected, PRP induced a significant

increase of calcium accumulation and of ALP activity compared with undifferentiated cells (Figure S3b,c), but no differences were observed between LG and HG (Figure S3b,c and Data S1).

To further investigate the effect of PRP on BFP–MSCs differentiated in high/low-glucose concentration, mRNA levels of *ALP*, *RUNX2*, and *COL1A1* were determined by qRT-PCR at Day 21 after induction of osteogenic differentiation (Figure 6a–c). As shown in Figure 6a, in LG, *ALP* mRNA levels similarly increased both in the presence and in the absence of PRP. At variance, in HG, PRP induced a significant increase of *ALP* expression levels compared with the control (Figure 6a). *RUNX2* and *COL1A1* mRNA levels increased in PRP-treated cells compared with untreated cells, either in LG and in HG (Figure 6b,c). Notably, in the presence of PRP, there was no more statistically significant difference in *ALP*, *RUNX2*, and *COL1A1* mRNA levels between cells differentiating in LG and HG (Figure 6a–c). Finally, protein levels of RUNX2 and Collagen 1 were significantly increased in the presence of PRP, with no difference between cells differentiated in LG or in HG (Figure 6d).
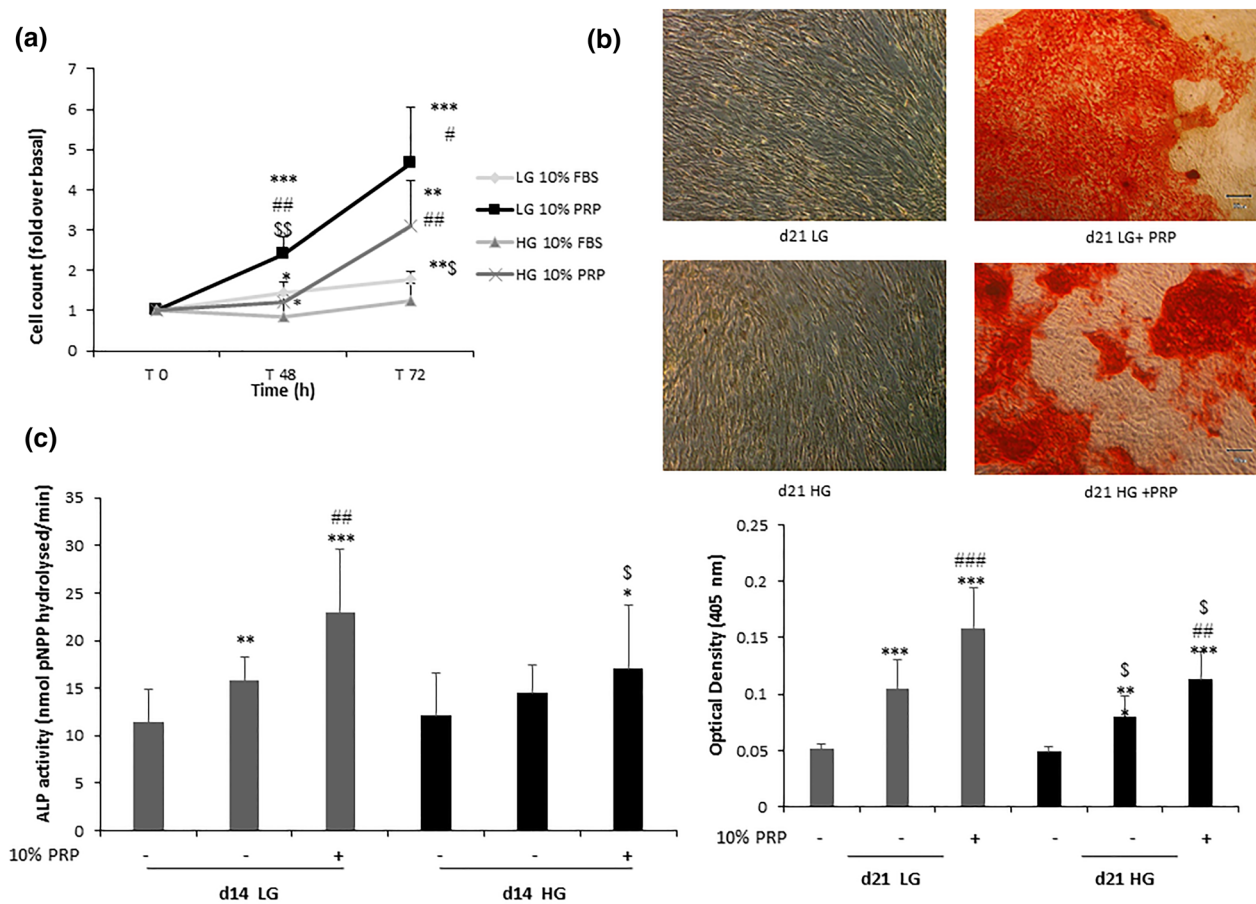
**FIGURE 5** Effect of PRP on BFP–MSC proliferation and differentiation in low-glucose (LG) and high-glucose (HG) medium. (a) BFP–MSCs were incubated with PRP gel (10% v/v in DMEM LG and HG without serum supplementation and DMEM LG and HG with serum) after 24 h from plating, for 48 and 72 h. Then, cells were counted as described in Section 2, and the results were reported as cell number relative to T0 ($^*p \leq 0.05$; $^{**}p \leq 0.01$; $^{***}p \leq 0.001$). Data in the graphs represent the mean ± SD of at least three experiments. Number sign ($^\#$) denotes statistical significance versus 10% PRP ($^\#p \leq 0.05$; $^{\#\#}p \leq 0.01$). Dollar sign ($^\$$) denotes statistical significance versus HG ($^\$p \leq 0.05$; $^{\$\$}p \leq 0.01$). (b and c) BFP–MSCs were cultured in osteogenic differentiation medium, in the presence or absence of PRP gel (10% v/v in DMEM LG and HG). Alizarin Red S representative images at 10× magnification (upper) and quantification (lower). Data in the graphs represent the mean ± SD of at least five experiments. Asterisk ($^*$) denotes statistical significance versus undifferentiated cells ($^{***}p \leq 0.001$). Number sign ($^\#$) denotes statistical significance versus cells differentiated without PRP ($^{\#\#}p \leq 0.01$; $^{\#\#\#}p \leq 0.001$). Dollar sign ($^\$$) denotes statistical significance versus LG ($^\$p \leq 0.05$). (b) ALP activity. Data in the graphs represent the mean ± SD of at least four experiments. Asterisk ($^*$) denotes statistical significance versus undifferentiated cells ($^*p \leq 0.05$; $^{**}p \leq 0.01$; $^{***}p \leq 0.001$). Number sign ($^\#$) denotes statistical significance versus cells differentiated without PRP ($^{\#\#}p \leq 0.01$). Dollar sign ($^\$$) denotes statistical significance versus LG ($^\$p \leq 0.05$) (c) [Colour figure can be viewed at wileyonlinelibrary.com]
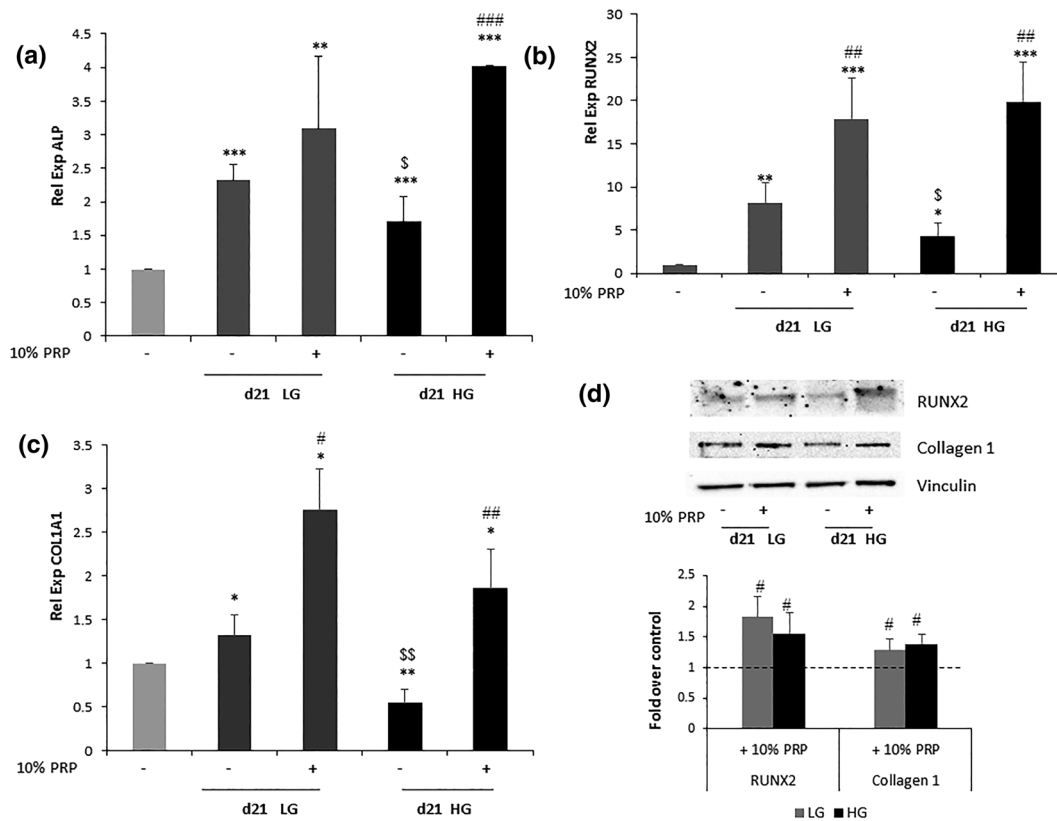
## 4 | DISCUSSION

The use of MSCs in regenerative medicine holds a great deal of promises. MSCs can be manipulated to obtain mature tissues and to facilitate correct organ rehabilitation. Their potential plasticity also represents a benefit for the reconstruction of wounded tissues (Shi et al., 2016). However, the availability of MSCs may be a limiting factor, due to the difficult accessibility of the main sources. According to previous reports (Broccaioli et al., 2013; Kishimoto, Honda, Momota, & Tran, 2018; Niada et al., 2013), here, we show that BFP contains MSCs, which can be isolated and cultured for several passages. They display all main markers of MSCs, which can be found in bone marrow and subcutaneous adipose tissue. Hence, they have a good capability

to differentiate toward both the adipogenic and the osteogenic lineage (Ardeshirylajimi et al., 2015; Ghaderi et al., 2018), providing a strong rationale for their use in maxillofacial surgery. Indeed, they have been adopted both for facilitating the healing of oral ulcers and for bone reconstruction procedures (Lee et al., 2017). Moreover, both harvesting and application of BFP into alveolar cavities or onto buccal soft tissues have proven to be safe and without any risk for the patient (Khojasteh & Sadeghi, 2016; Khojasteh et al., 2017).

However, it should be taken into account that systemic diseases, such as diabetes, may influence the properties of MSCs (Tobita et al., 2015) and functionally compromised MSCs may be therapeutically ineffective. The effect of metabolic derangement may also be different in diverse fat depots and may depend on the timing of cell

**FIGURE 6** Effect of PRP on BFP–MSC osteogenic markers in low-glucose (LG) and high-glucose (HG) medium. BFP–MSCs were cultured in osteogenic differentiation medium, in the presence or absence of PRP gel (10% v/v in DMEM LG and HG). *ALP* (a), *RUNX2* (b), and *COL1A1* (c) mRNA levels were determined by real-time RT-PCR analysis. Data have been normalized on PPIA as internal standard. Bars show the mRNA levels relative to undifferentiated control at Day 0. Asterisk (*) denotes statistical significance versus undifferentiated cells (*$p \leq 0.05$; **$p \leq 0.01$; ***$p \leq 0.001$). Number sign (#) denotes statistical significance versus cells differentiated without PRP (##$p \leq 0.01$; ###$p \leq 0.001$). Dollar sign ($) denotes statistical significance versus LG ($$p \leq 0.05$; $$$p \leq 0.01$). (d) Cell lysates (30-μg protein/sample) were blotted with RUNX2 and Collagen 1 antibodies. To ensure the equal protein transfer, membranes were blotted with vinculin antibodies. Filters were revealed by ECL and autoradiography. The autoradiographs shown are representative of three independent experiments. Densitometric analysis has been performed on autoradiographs. Bars show the ratio RUNX2/vinculin and Collagen 1/vinculin protein levels relative to control (cells at Day 21 without PRP), represented as dotted line. Data in the graphs represent the mean ± SD of three experiments. Asterisk (*) denotes statistical significance versus control (*$p \leq 0.05$)

exposure (Ferrer-Lorente, Bejar, & Badimon, 2014). For this reason, different groups have investigated the effects of high-glucose concentrations on MSCs, with conflicting results. Most of the studies have been performed on bone marrow MSCs (BM-MSCs) and show that glucose may either increase, either reduce, and either have no effect on cell proliferation and osteogenic differentiation (Hankamolsiri et al., 2016; Wang et al., 2013). For instance, no consistent effect was seen on proliferation of BM-MSCs in short-term exposure (4 days) to 25-mM glucose, whereas in long-term cultures (4 weeks), a slight but significant decrease of cell proliferation was observed (Li et al., 2007). Visceral MSCs exposed to high glucose for 14 days display an increase of proliferation and of dedifferentiation markers (Dentelli et al., 2013). Our results on sc-MSCs are in agreement with previous reports (Dhanasekaran, Indumathi, Rajkumar, & Sudarsanam, 2013), indicating that glucose does not impair cell proliferation and induces a slight increase in osteogenic differentiation. However, we cannot exclude

that a longer period of treatment with high glucose may have different effects. Until now, no one has investigated the effects of glucose on BFP–MSCs. This is an important gap in literature because dental implant therapy in patients having diabetes is still considered a relative contraindication. However, if the plasma glucose levels are normal or close to normal, the higher implant failure rate observed in diabetic patients tends to be closer to that observed in nondiabetic individuals (Ladha et al., 2017).

Here, we show for the first time that exposure of BFP–MSCs to high-glucose concentrations, consistent with glucose levels detectable in hyperglycemia, impairs cell growth and osteogenic differentiation potential. This observation suggests that excessive glucose may be detrimental for bone formation, also when MSCs are used for reconstruction procedures. Thus, in diabetic individuals, a tight glycemic control is certainly needed for bone homeostasis and for a better outcome of regeneration approaches.

Among the strategies to enhance tissue regeneration and bone formation, the use of platelet-derived products plays a major role. They have found applications in several fields of the regenerative medicine, from the reconstructive to the esthetic surgery and from the orthopedics to the ophthalmology (Mulder, Lee, & Jeppesen, 2012). At cellular level, we and others have shown that PRP enhances the proliferation, the motility, and the osteogenic differentiation of subcutaneous adipose tissue MSCs and of dental stem cells (D'Esposito et al., 2015; Otero, Carrillo, Calvo-Guirado, Villamil, & Delgado-Ruiz, 2017; Scioli, Bielli, Gentile, Cervelli, & Orlandi, 2017; Tajima, Tobita, & Mizuno, 2018; Tajima, Tobita, Orbay, Hyakusoku, & Mizuno, 2015). The basic principle is the release of growth factors and cytokines by activated platelets, which may sustain MSC growth and differentiation. For instance, PRP releases large amount of PDGF, VEGF, TGF-β1, and CCL5 (Lacci & Dardik, 2010; Lubkowska et al., 2012; Passaretti et al., 2014), all factors promoting MSC proliferation and osteogenic differentiation (Ding et al., 2010; Huang, Ren, Ma, Smith, & Goodman, 2010; Hung et al., 2015; Liu et al., 2014; Zhao & Hantash, 2011). Moreover, PRP addition on MSC cultures also increases the growth factor release (IGF-1, TGF-β1, and VEGF) by MSC themselves (Tajima et al., 2015).

We now provide evidence that PRP can also promote survival and growth of BFP–MSCs also in the presence of high-glucose concentrations. This finding implies that, even in a "diabetic milieu," PRP might be a useful tool to enrich the amount of MSCs available for the purpose of bone regeneration. An unsolved question remains about the use of autologous PRP in diabetic patients. in vitro studies have shown a number of anomalies in the mechanisms of action of platelets in diabetic subjects. These anomalies lead to hyper-reactive platelets (Vinik, Erbas, Park, Nolan, & Pittenger, 2001). However, as compared with nondiabetic controls, angiogenic activities of platelets remain unaltered in T2D patients (Miao, Zhang, Huang, & Li, 2016). Some authors have also found that PRP from diabetic patients releases more VEGF and increases proliferation and migration of endothelial cells at larger extent, compared with PRP from healthy donors (Etulain et al., 2018; Karina et al., 2019). Notably, solid evidence supports the use of autologous PRP for the treatment of diabetic foot ulcers (Hirase, Ruff, Surani, & Ratnani, 2018).

Thus, our data are consistent with the hypothesis that hyperglycemia impairs the function of BFP–MSCs, reducing their growth and osteogenic differentiation potential. On the other end, PRP enhances BFP–MSC growth, without impairing osteogenic differentiation capability. Interestingly, PRP treatment also rescues osteogenic differentiation in high-glucose concentrations, suggesting that platelet products may at least partially compensate for detrimental glucose effect. More work needs to be done to elucidate the molecular mechanisms by which MSCs isolated from diverse sources differently respond to glucose stimuli and to PRP. Nevertheless, PRP has been successfully used for osteogenic tissue engineering approaches (Otero et al., 2017; Scioli et al., 2017). Because of its relative ease of preparation and safety of use, PRP (or other similar tools) could be considered as a relevant supplementation for sources of MSCs in tissue regeneration procedures, even in the presence of comorbidities such as diabetes.

## CONFLICT OF INTEREST

The authors have no conflict of interest to declare.

## AUTHOR CONTRIBUTIONS

M. L. and V. D. E. conceived, designed the experiments, and analyzed the data. M. R. A., S. C., and T. M. performed and analyzed the data based on cell cultures. S. M. and P. L. were involved in PRP study (enrollment of patients, characterization of PRP, and PRP–gel preparation). G. M., L. F., J. C. S., and R. G. enrolled patients undergoing to maxillary bone reconstruction interventions and obtained BFP. F. B., F. O., and G. S. analyzed the data and wrote the manuscript. P. F. and R. G. coordinated the study. We confirm that all authors have approved the manuscript and agree with the submission.

## ORCID

*Pietro Formisano* 🔟 https://orcid.org/0000-0001-7020-6870

## REFERENCES

Ardeshirylajimi, A., Mossahebi-Mohammadi, M., Vakilian, S., Langroudi, L., Seyedjafari, E., Atashi, A., & Soleimani, M. (2015). Comparison of osteogenic differentiation potential of human adult stem cells loaded on bioceramic-coated electrospun poly(L-lactide) nanofibres. *Cell Proliferation*, *48*(1), 47–58. https://doi.org/10.1111/cpr.12156

Ariemma, F., D'Esposito, V., Liguoro, D., Oriente, F., Cabaro, S., Liotti, A., ... Valentino, R. (2016). Low-dose bisphenol-A impairs adipogenesis and generates dysfunctional 3T3-L1 adipocytes. *PLoS ONE*, *11*(3), e0150762. https://doi.org/10.1371/journal.pone.0150762

Broccaioli, E., Niada, S., Rasperini, G., Ferreira, L. M., Arrigoni, E., Yenagi, V., & Brini, A. T. (2013). Mesenchymal stem cells from Bichat's fat pad: in vitro comparison with adipose-derived stem cells from subcutaneous tissue. *Biores Open Access*, *2*(2), 107–117. https://doi.org/10.1089/biores.2012.0291

Burnouf, T., Goubran, H. A., Chen, T. M., Ou, K. L., El-Ekiaby, M., & Radosevic, M. (2013). Blood-derived biomaterials and platelet growth factors in regenerative medicine. *Blood Reviews*, *27*(2), 77–89. https://doi.org/10.1016/j.blre.2013.02.001

Cabaro, S., D'Esposito, V., Gasparro, R., Borriello, F., Granata, F., Mosca, G., ... Riccitiello, F. (2018). White cell and platelet content affects the release of bioactive factors in different blood-derived scaffolds. *Platelets*, *29*(5), 463–467. https://doi.org/10.1080/09537104.2017.1319046

Caplan, A. I. (2007). Adult mesenchymal stem cells for tissue engineering versus regenerative medicine. *Journal of Cellular Physiology*, *213*(2), 341–347. https://doi.org/10.1002/jcp.21200

Choi, H. J., & Lee, J. B. (2016). Obliteration of recurrent large dentigerous cyst using bilateral buccal fat pad sling flaps. *The Journal of Craniofacial Surgery*, *27*(5), e465–e468. https://doi.org/10.1097/SCS.0000000000002780

Dalle Carbonare, L., Innamorati, G., & Valenti, M. T. (2012). Transcription factor Runx2 and its application to bone tissue engineering. *Stem Cell Reviews and Reports*, *8*(3), 891–897. https://doi.org/10.1007/s12015-011-9337-4

Dentelli, P., Barale, C., Togliatto, G., Trombetta, A., Olgasi, C., Gili, M., … Brizzi, M. F. (2013). A diabetic milieu promotes OCT4 and NANOG production in human visceral-derived adipose stem cells. *Diabetologia*, *56*(1), 173–184. https://doi.org/10.1007/s00125-012-2734-7

D'Esposito, V., Passaretti, F., Hammarstedt, A., Liguoro, D., Terracciano, D., Molea, G., … Formisano, P. (2012). Adipocyte-released insulin-like growth factor-1 is regulated by glucose and fatty acids and controls breast cancer cell growth in vitro. *Diabetologia*, *55*(10), 2811–2822. https://doi.org/10.1007/s00125-012-2629-7

D'Esposito, V., Passaretti, F., Perruolo, G., Ambrosio, M. R., Valentino, R., Oriente, F., … Formisano, P. (2015). Platelet-rich plasma increases growth and motility of adipose tissue-derived mesenchymal stem cells and controls adipocyte secretory function. *Journal of Cellular Biochemistry*, *116*(10), 2408–2418. https://doi.org/10.1002/jcb.25235

Dhanasekaran, M., Indumathi, S., Rajkumar, J. S., & Sudarsanam, D. (2013). Effect of high glucose on extensive culturing of mesenchymal stem cells derived from subcutaneous fat, omentum fat and bone marrow. *Cell Biochemistry and Function*, *31*(1), 20–29. https://doi.org/10.1002/cbf.2851

Ding, W., Knox, T. R., Tschumper, R. C., Wu, W., Schwager, S. M., Boysen, J. C., … Kay, N. E. (2010). Platelet-derived growth factor (PDGF)–PDGF receptor interaction activates bone marrow-derived mesenchymal stromal cells derived from chronic lymphocytic leukemia: Implications for an angiogenic switch. *Blood*, *116*(16), 2984–2993. https://doi.org/10.1182/blood-2010-02-269894

Etulain, J., Mena, H. A., Meiss, R. P., Frechtel, G., Gutt, S., Negrotto, S., & Schattner, M. (2018). An optimised protocol for platelet-rich plasma preparation to improve its angiogenic and regenerative properties. *Scientific Reports*, *8*(1), 1513. https://doi.org/10.1038/s41598-018-19419-6

Farre-Guasch, E., Marti-Page, C., Hernandez-Alfaro, F., Klein-Nulend, J., & Casals, N. (2010). Buccal fat pad, an oral access source of human adipose stem cells with potential for osteochondral tissue engineering: An in vitro study. *Tissue Engineering. Part C, Methods*, *16*(5), 1083–1094. https://doi.org/10.1089/ten.TEC.2009.0487

Ferrer-Lorente, R., Bejar, M. T., & Badimon, L. (2014). Notch signaling pathway activation in normal and hyperglycemic rats differs in the stem cells of visceral and subcutaneous adipose tissue. *Stem Cells and Development*, *23*(24), 3034–3048. https://doi.org/10.1089/scd.2014.0070

Fijany, A., Sayadi, L. R., Khoshab, N., Banyard, D. A., Shaterian, A., Alexander, M., … Widgerow, A. D. (2019). Mesenchymal stem cell dysfunction in diabetes. *Molecular Biology Reports*, *46*(1), 1459–1475. https://doi.org/10.1007/s11033-018-4516-x

Ghaderi, H., Razmkhah, M., Kiany, F., Chenari, N., Haghshenas, M. R., & Ghaderi, A. (2018). Comparison of osteogenic and chondrogenic differentiation ability of buccal fat pad derived mesenchymal stem cells and gingival derived cells. *J Dent (Shiraz)*, *19*(2), 124–131.

Giacco, F., Perruolo, G., D'Agostino, E., Fratellanza, G., Perna, E., Misso, S., … Formisano, P. (2006). Thrombin-activated platelets induce proliferation of human skin fibroblasts by stimulating autocrine production of insulin-like growth factor-1. *The FASEB Journal*, *20*(13), 2402–2404. https://doi.org/10.1096/fj.06-6104fje

Hankamolsiri, W., Manochantr, S., Tantrawatpan, C., Tantikanlayaporn, D., Tapanadechopone, P., & Kheolamai, P. (2016). The effects of high glucose on adipogenic and osteogenic differentiation of gestational tissue-derived MSCs. *Stem Cells International*, *2016*, 9674614. https://doi.org/10.1155/2016/9674614

Hirase, T., Ruff, E., Surani, S., & Ratnani, I. (2018). Topical application of platelet-rich plasma for diabetic foot ulcers: A systematic review. *World Journal of Diabetes*, *9*(10), 172–179. https://doi.org/10.4239/wjd.v9.i10.172

Huang, Z., Ren, P. G., Ma, T., Smith, R. L., & Goodman, S. B. (2010). Modulating osteogenesis of mesenchymal stem cells by modifying growth factor availability. *Cytokine*, *51*(3), 305–310. https://doi.org/10.1016/j.cyto.2010.06.002

Hung, B. P., Hutton, D. L., Kozielski, K. L., Bishop, C. J., Naved, B., Green, J. J., … Grayson, W. L. (2015). Platelet-derived growth factor bb enhances osteogenesis of adipose-derived but not bone marrow-derived mesenchymal stromal/stem cells. *Stem Cells*, *33*(9), 2773–2784. https://doi.org/10.1002/stem.2060

Isakson, P., Hammarstedt, A., Gustafson, B., & Smith, U. (2009). Impaired preadipocyte differentiation in human abdominal obesity: Role of Wnt, tumor necrosis factor-alpha, and inflammation. *Diabetes*, *58*(7), 1550–1557. https://doi.org/10.2337/db08-1770

Karina, K. A. W., Sobariah, S., Rosliana, I., Rosadi, I., Widyastuti, T., Afini, I., … Pawitan, J. A. (2019). Evaluation of platelet-rich plasma from diabetic donors shows increased platelet vascular endothelial growth factor release. *Stem Cell Investigation*, *6*, 1–6. https://doi.org/10.21037/sci.2019.10.02

Khojasteh, A., Kheiri, L., Behnia, H., Tehranchi, A., Nazeman, P., Nadjmi, N., & Soleimani, M. (2017). Lateral ramus cortical bone plate in alveolar cleft osteoplasty with concomitant use of buccal fat pad derived cells and autogenous bone: Phase I clinical trial. *BioMed Research International*, *2017*, 6560234. https://doi.org/10.1155/2017/6560234

Khojasteh, A., & Sadeghi, N. (2016). Application of buccal fat pad-derived stem cells in combination with autogenous iliac bone graft in the treatment of maxillomandibular atrophy: A preliminary human study. *International Journal of Oral and Maxillofacial Surgery*, *45*(7), 864–871. https://doi.org/10.1016/j.ijom.2016.01.003

Kishimoto, N., Honda, Y., Momota, Y., & Tran, S. D. (2018). Dedifferentiated fat (DFAT) cells: A cell source for oral and maxillofacial tissue engineering. *Oral Diseases*, *24*(7), 1161–1167. https://doi.org/10.1111/odi.12832

Lacci, K. M., & Dardik, A. (2010). Platelet-rich plasma: Support for its use in wound healing. *The Yale Journal of Biology and Medicine*, *83*(1), 1–9.

Ladha, K., Sharma, A., Tiwari, B., & Bukya, D. N. (2017). Bone augmentation as an adjunct to dental implant rehabilitation in patients with diabetes mellitus: A review of literature. *Natl J Maxillofac Surg*, *8*(2), 95–101. https://doi.org/10.4103/njms.NJMS_16_17

Lanza, D., Perna, A. F., Oliva, A., Vanholder, R., Pletinck, A., Guastafierro, S., … Ingrosso, D. (2015). Impact of the uremic milieu on the osteogenic potential of mesenchymal stem cells. *PLoS ONE*, *10*(1), e0116468. https://doi.org/10.1371/journal.pone.0116468

Lee, D. Y., Kim, H. B., Shim, I. K., Kanai, N., Okano, T., & Kwon, S. K. (2017). Treatment of chemically induced oral ulcer using adipose-derived mesenchymal stem cell sheet. *Journal of Oral Pathology & Medicine*, *46*(7), 520–527. https://doi.org/10.1111/jop.12517

Li, Y. M., Schilling, T., Benisch, P., Zeck, S., Meissner-Weigl, J., Schneider, D., … Ebert, R. (2007). Effects of high glucose on mesenchymal stem cell proliferation and differentiation. *Biochemical and Biophysical Research Communications*, *363*(1), 209–215. https://doi.org/10.1016/j.bbrc.2007.08.161

Liu, Y. C., Kao, Y. T., Huang, W. K., Lin, K. Y., Wu, S. C., Hsu, S. C., … Lu, J. (2014). CCL5/RANTES is important for inducing osteogenesis of human mesenchymal stem cells and is regulated by dexamethasone. *Bioscience Trends*, *8*(3), 138–143. https://doi.org/10.5582/bst.2014.01047

Lubkowska, A., Dolegowska, B., & Banfi, G. (2012). Growth factor content in PRP and their applicability in medicine. *Journal of Biological Regulators and Homeostatic Agents*, *26*(2 Suppl 1), 3S–22S.

Miao, X., Zhang, W., Huang, Z., & Li, N. (2016). Unaltered angiogenesis-regulating activities of platelets in mild type 2 diabetes mellitus despite

a marked platelet hyperreactivity. *PLoS ONE*, *11*(9), e0162405. https://doi.org/10.1371/journal.pone.0162405

Morris, H. F., Ochi, S., & Winkler, S. (2000). Implant survival in patients with type 2 diabetes: Placement to 36 months. *Annals of Periodontology*, *5*(1), 157–165. https://doi.org/10.1902/annals.2000.5.1.157

Mulder, G. D., Lee, D. K., & Jeppesen, N. S. (2012). Comprehensive review of the clinical application of autologous mesenchymal stem cells in the treatment of chronic wounds and diabetic bone healing. *International Wound Journal*, *9*(6), 595–600. https://doi.org/10.1111/j.1742-481X.2011.00922.x

Niada, S., Ferreira, L. M., Arrigoni, E., Addis, A., Campagnol, M., Broccaioli, E., & Brini, A. T. (2013). Porcine adipose-derived stem cells from buccal fat pad and subcutaneous adipose tissue for future pre-clinical studies in oral surgery. *Stem Cell Research & Therapy*, *4*(6), 148. https://doi.org/10.1186/scrt359

Otero, L., Carrillo, N., Calvo-Guirado, J. L., Villamil, J., & Delgado-Ruiz, R. A. (2017). Osteogenic potential of platelet-rich plasma in dental stem-cell cultures. *The British Journal of Oral & Maxillofacial Surgery*, *55*(7), 697–702. https://doi.org/10.1016/j.bjoms.2017.05.005

Passaretti, F., Tia, M., D'Esposito, V., De Pascale, M., Del Corso, M., Sepulveres, R., ... Sammartino, G. (2014). Growth-promoting action and growth factor release by different platelet derivatives. *Platelets*, *25*(4), 252–256. https://doi.org/10.3109/09537104.2013.809060

Ramirez-Zacarias, J. L., Castro-Munozledo, F., & Kuri-Harcuch, W. (1992). Quantitation of adipose conversion and triglycerides by staining intracytoplasmic lipids with Oil Red O. *Histochemistry*, *97*(6), 493–497. https://doi.org/10.1007/bf00316069

Retzepi, M., Calciolari, E., Wall, I., Lewis, M. P., & Donos, N. (2018). The effect of experimental diabetes and glycaemic control on guided bone regeneration: Histology and gene expression analyses. *Clinical Oral Implants Research*, *29*(2), 139–154. https://doi.org/10.1111/clr.13031

Rezai Rad, M., Bohloli, M., Akhavan Rahnama, M., Anbarlou, A., Nazeman, P., & Khojasteh, A. (2017). Impact of tissue harvesting sites on the cellular behaviors of adipose-derived stem cells: Implication for bone tissue engineering. *Stem Cells International*, *2017*, 2156478. https://doi.org/10.1155/2017/2156478

Salehi-Nik, N., Rezai Rad, M., Kheiri, L., Nazeman, P., Nadjmi, N., & Khojasteh, A. (2017). Buccal fat pad as a potential source of stem cells for bone regeneration: A literature review. *Stem Cells International*, *2017*, 8354640. https://doi.org/10.1155/2017/8354640

Schwartz-Arad, D., Levin, L., & Sigal, L. (2005). Surgical success of intraoral autogenous block onlay bone grafting for alveolar ridge augmentation. *Implant Dentistry*, *14*(2), 131–138. https://doi.org/10.1097/01.id.0000165031.33190.0d

Scioli, M. G., Bielli, A., Gentile, P., Cervelli, V., & Orlandi, A. (2017). Combined treatment with platelet-rich plasma and insulin favours chondrogenic and osteogenic differentiation of human adipose-derived stem cells in three-dimensional collagen scaffolds. *Journal of Tissue Engineering and Regenerative Medicine*, *11*(8), 2398–2410. https://doi.org/10.1002/term.2139

Shi, R., Jin, Y., Cao, C., Han, S., Shao, X., Meng, L., ... Li, M. (2016). Localization of human adipose-derived stem cells and their effect in repair of diabetic foot ulcers in rats. *Stem Cell Research & Therapy*, *7*(1), 155. https://doi.org/10.1186/s13287-016-0412-2

Stewart, J. E., Wager, K. A., Friedlander, A. H., & Zadeh, H. H. (2001). The effect of periodontal treatment on glycemic control in patients with type 2 diabetes mellitus. *Journal of Clinical Periodontology*, *28*(4), 306–310. https://doi.org/10.1034/j.1600-051x.2001.028004306.x

Tajima, S., Tobita, M., & Mizuno, H. (2018). Bone regeneration with a combination of adipose-derived stem cells and platelet-rich plasma. *Methods in Molecular Biology*, *1773*, 261–272. https://doi.org/10.1007/978-1-4939-7799-4_20

Tajima, S., Tobita, M., Orbay, H., Hyakusoku, H., & Mizuno, H. (2015). Direct and indirect effects of a combination of adipose-derived stem cells and platelet-rich plasma on bone regeneration. *Tissue Engineering.*

*Part A*, *21*(5–6), 895–905. https://doi.org/10.1089/ten.TEA.2014.0336

Tobita, M., Tajima, S., & Mizuno, H. (2015). Adipose tissue-derived mesenchymal stem cells and platelet-rich plasma: Stem cell transplantation methods that enhance stemness. *Stem Cell Research & Therapy*, *6*, 215. https://doi.org/10.1186/s13287-015-0217-8

Vinik, A. I., Erbas, T., Park, T. S., Nolan, R., & Pittenger, G. L. (2001). Platelet dysfunction in type 2 diabetes. *Diabetes Care*, *24*(8), 1476–1485. https://doi.org/10.2337/diacare.24.8.1476

van de Vyver, M. (2017). Intrinsic mesenchymal stem cell dysfunction in diabetes mellitus: Implications for autologous cell therapy. *Stem Cells and Development*, *26*(14), 1042–1053. https://doi.org/10.1089/scd.2017.0025

Wang, J., Wang, B., Li, Y., Wang, D., Lingling, E., Bai, Y., & Liu, H. (2013). High glucose inhibits osteogenic differentiation through the BMP signaling pathway in bone mesenchymal stem cells in mice. *EXCLI Journal*, *12*, 584–597.

Xu, F. T., Li, H. M., Yin, Q. S., Liang, Z. J., Huang, M. H., Chi, G. Y., ... Nan, H. (2015). Effect of activated autologous platelet-rich plasma on proliferation and osteogenic differentiation of human adipose-derived stem cells in vitro. *American Journal of Translational Research*, *7*(2), 257–270.

Yousuf, S., Tubbs, R. S., Wartmann, C. T., Kapos, T., Cohen-Gadol, A. A., & Loukas, M. (2010). A review of the gross anatomy, functions, pathology, and clinical uses of the buccal fat pad. *Surgical and Radiologic Anatomy*, *32*(5), 427–436. https://doi.org/10.1007/s00276-009-0596-6

Zhao, L., & Hantash, B. M. (2011). TGF-beta1 regulates differentiation of bone marrow mesenchymal stem cells. *Vitamins and Hormones*, *87*, 127–141. https://doi.org/10.1016/B978-0-12-386015-6.00042-1

## SUPPORTING INFORMATION

Additional supporting information may be found online in the Supporting Information section at the end of this article.

Figure S1. *Effect of glucose on sc-MSC proliferation and differentiation.* A) sc-MSCs were incubated in DMEM 5.5 mM glucose (Low glucose; LG) and 25 mM glucose (High glucose; HG) supplemented with 10% FBS or 0.25% BSA for 48 h and 72 h. Then, cells were counted and the results reported as cell number relative to T0. Data in the graphs represent the mean ± SD of at least 3 experiments.* denotes statistical significance over T0 (* $p ≤ 0.05$; ** $p ≤ 0.01$; *** $p ≤ 0.001$). # denotes statistical significance versus 10% FBS (### $p ≤ 0.001$). sc-MSCs were cultured in osteogenic differentiation medium in LG or HG. B) ARS representative images at 10X magnification (upper) and quantification (lower).. Data in the graphs represent the mean ± SD of at least 3 experiments. * denotes statistical significance versus undifferentiated cells (*** $p ≤ 0.001$). $ denotes statistical significance versus LG ($ $p ≤ 0.05$; $$$ $p ≤ 0.001$). C) ALP activity. Data in the graphs represent the mean ± SD of at least 4 experiments. * denotes statistical significance versus undifferentiated cells (** $p ≤ 0.01$).

Figure S2. *Effect of PRP on BFP-MSC proliferation and differentiation.* A) BFP-MSCs serum-starved for 9 h and then incubated with PRP gel (10% vol/vol in DMEM F12 1:1) for 48 h and 72 h without serum supplementation (MEDIUM BSA). As control, BFP-MSCs were incubated with DMEM F12 (1:1) without serum supplementation. Then, cells were counted as described in Materials and Methods and the results reported as cell number relative to T0. Data in the graphs represent the mean ± SD of at least 4 experiments.* denotes statistical

significance over T0 (* $p \leq 0.05$; *** $p \leq 0.001$). # denotes statistical significance versus 10% PRP (### $p \leq 0.001$); B) BFP-MSCs were cultured in osteogenic differentiation medium as described in Materials and Methods, ALP mRNA levels were determined by real-time RT-PCR analysis. Data have been normalized on PPIA as internal standard. Bars show the mRNA levels relative to undifferentiated control. * denotes statistically significant values over undifferentiated cells at d0 (** $p \leq 0.01$, *** $p \leq 0.001$).

Figure S3. *Effect of PRP on sc-MSC proliferation and differentiation in LG and HG medium.* A) sc-MSCs were incubated with PRP gel (10% vol/vol in DMEM LG and HG without serum supplementation and DMEM LG and HG with serum) after 24 h from plating for 48 h and 72 h. Then, cells were counted as described in Materials and Methods and the results reported as cell number relative to T0 (* $p \leq 0.05$; ** $p \leq 0.01$; *** $p \leq 0.001$). # denotes statistical significance versus 10% PRP (# $p \leq 0.05$; ## $p \leq 0.01$; ### $p \leq 0.001$). Data in the graphs represent the mean ± SD of at least 3 experiments. B-C) sc-MSCs were cultured in osteogenic differentiation medium in presence or absence of PRP gel (10% vol/vol in DMEM LG and HG). ARS representative images at 10X magnification (upper) and quantification (lower). Data in the graphs represent the mean ± SD of at least 3 experiments. * denotes statistical significance versus undifferentiated cells (** $p \leq 0.01$; *** $p \leq 0.001$). # denotes statistical significance versus cells differentiated without PRP (## $p \leq 0.01$). $ denotes statistical significance versus LG ($$$ $p \leq 0.001$) (B). ALP activity. Data in the graphs represent the mean ± SD of at least 4 experiments. * denotes statistical significance versus undifferentiated cells (** $p \leq 0.01$; *** $p \leq 0.001$) (C).

Data S1. Supporting Information